Box diagram in the elastic electron-proton scattering

Dmitry Borisyuk and Alexander Kobushkin*
Bogolyubov Institute for Theoretical Physics, Metrologicheskaya street 14-B, 03143 Kiev, Ukraine
(Received 30 June 2006; published 19 December 2006)

We present an evaluation of the box diagram for elastic *ep* scattering with the proton in the intermediate state. Using analytic properties of the proton form factors we express the amplitude via a twofold integral that involves the form factors in the spacelike region only. Therefore experimentally measured form factors can be used in the calculations directly. The numerical calculation is done with the form factors extracted by Rosenbluth separation, as well as polarization transfer method. The dependence of the results on the form factor choice is small for $Q^2 \lesssim 6\ \mathrm{GeV}^2$ but becomes sizable at higher Q^2.

DOI: 10.1103/PhysRevC.74.065203 PACS number(s): 25.30.Bf, 12.38.−t, 14.20.Dh, 24.70.+s

I. INTRODUCTION

The study of elastic electron-proton scattering,

$$e^- + p \to e^- + p, \tag{1}$$

provides an important source of information about the proton structure. In first-order perturbation theory (PT) or the Born approximation the reaction amplitude

$$\mathcal{M}_{\mathrm{Born}} = \frac{4\pi\alpha}{q^2}\bar{u}'\gamma_\mu u \cdot \bar{U}'\Gamma^\mu(q)U \tag{2}$$

is expressed in terms of Dirac and Pauli proton form factors (FFs), F_1 and F_2,

$$\Gamma_\mu(q) = F_1(q^2)\gamma_\mu - F_2(q^2)[\gamma_\mu, \gamma_\nu]\frac{q^\nu}{4M}, \tag{3}$$

where u, U, u', and U' are 4-spinors of incoming and outgoing particles, $\alpha \approx 1/137$ is fine-structure constant, and q is the momentum transfer from the electron to the proton. The linear combinations $G_E = F_1 + \frac{q^2}{4M^2}F_2$ and $G_M = F_1 + F_2$, called the electric and magnetic FFs, are also widely used.

For many years it was common practice to extract FFs by the Rosenbluth separation method. The FFs obtained by this method obey with good accuracy $G_E/G_M = \mathrm{const}$ for $0 < Q^2 \lesssim 6\ \mathrm{GeV}^2$ ($Q^2 \equiv -q^2$). However, since the year 2000, a series of experiments has been done using an alternative, polarization transfer method [1]. These experiments yielded strikingly different results: The G_E/G_M ratio decreased linearly with Q^2. Because both methods are based on the Born approximation, the reason for this discrepancy is likely to be the neglected higher order PT terms. There are two types of second-order Feynman diagrams: diagrams involving an exchange of only one virtual photon (vacuum polarization or vertex corrections) and two-photon exchange or box diagrams [Fig. 1(a)]. The portion of the amplitude coming from one-photon exchange diagrams has a structure similar to Eq. (2) (certainly with another functions in place of F_1 and F_2) and cannot lead to the discrepancy between the two methods. Such diagrams are usually taken into account in experimental analyses.

Therefore the two-photon exchange diagram plays the key role in understanding the experimental results and extracting correct FF values.

The lower part of the diagram represents the doubly virtual Compton scattering (VVCS) off the proton. The amplitude of VVCS has two poles, which are due to a single proton in the intermediate state. The contribution of these poles to the box diagram is called the elastic contribution. Similar contributions appear from $\Delta(1232)$ and other resonances (Fig. 1). In the present paper we study the elastic contribution only [diagrams shown in Figs. 1(b) and 1(c), which we later call box (in the narrow sense) and x-box diagrams]. We also believe that the method derived here can be applied, with minor modifications, to the contributions of resonances. This will be the subject of a separate paper.

In previously published papers the box diagram was calculated in several, more or less approximate ways.

The first is the soft-photon approximation used in Tsai's paper [2] (and also in Ref. [3]). It is assumed that the main contribution to the loop integral comes from the $q_1 \approx 0$, $q_2 \approx q$ and $q_1 \approx q$, $q_2 \approx 0$ regions, because the integrand is strongly peaked at these points owing to the infrared (IR) singularity. However, only the IR divergent part (which exactly cancels in the final answer) can be calculated in such a way. Instead, we are interested here in the IR finite part, and it is by no means obvious that the main contribution to it comes from the same regions.

In the second way, which may be called the "hard-photon approximation," one assumes the most important region to be $q_1 \approx q_2 \approx q/2$ [4]. This may be a reasonable assumption; however, we believe it needs justification. In Ref. [4], after the approximation is made the loop integral becomes divergent and an ultraviolet cutoff is inserted by hand.

In the third group of papers the loop integral was calculated exactly, however with use of the special FF parametrization, monopole FF in Ref. [5] and the sum of monopoles in Ref. [6],

$$F_{1,2}(t) = \sum_i \frac{n_i}{d_i - t}, \tag{4}$$

where n_i and d_i are fitted constants. Because of this simple form, the resulting integrals are expressed through four- and

*Electronic address: kobushkin@bitp.kiev.ua

 ©2006 The American Physical Society

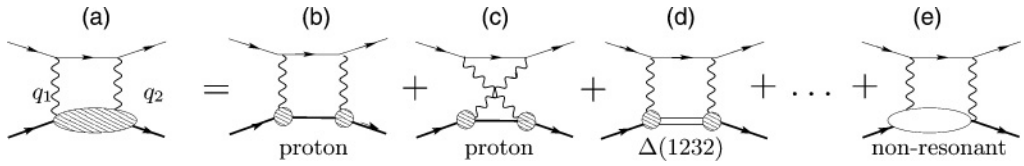

FIG. 1. Two-photon exchange for elastic *ep* scattering.

three-point functions, which were calculated numerically by using a computer program.

However, such a calculation has the following problem. Since the FFs, entering the integral are not known from first principles, we must use some model for them or fit to experiment.[1] The problem is that only the $t < 0$ region is accessible for the scattering experiments. Whereas the $t > 4M^2$ region can, in principle, be studied in the $e^- + e^+ \to p + \tilde{p}$ reaction, the unphysical region $0 < t < 4M^2$ is completely inaccessible. But the loop integral involves FFs in the timelike region ($t > 0$) as well. A natural question arises: How does the (largely unknown) FF behavior for $t > 0$ influence the total result. In particular, the parametrization used in Ref. [6] does not even roughly reproduce FFs in the $t > 0$ region. Indeed, unitarity requires that FFs have poles at $t = m_V^2$, where the m_V are masses of vector mesons, namely ρ, ω, and φ mesons (neglecting their widths). But the numerical values given in Ref. [6] strongly differ from these masses. So, the fit is not suitable for $t > 0$ and the results of Ref. [6] cannot be considered reliable before we answer the aforementioned question.

In the present paper we calculate the box and x-box diagrams in the most rigorous way. First, in contrast to the method of Refs. [2–4] we evaluate all integrals exactly, without any restriction of the integration domain. Second, in contrast to what was done in Refs. [5,6] we do not use any special assumptions on the FF's functional form. We perform the analytical integration to the maximal possible extent, resulting in

$$\mathcal{M}_{\substack{\text{box}\\ \text{x box}}} = \sum_{i,j=1}^{2} \int_{t_1,t_2 \leqslant 0} \mathcal{K}_{ij}(t_1,t_2) F_i(t_1) F_j(t_2) dt_1 dt_2, \quad (5)$$

where $\mathcal{K}_{ij}(t_1, t_2)$ is explicitly known. During the derivation of Eq. (5) we perform Wick rotation of the integration path, which is possible because of FF analyticity. As a result, the integration is done over negative t_1 and t_2 only. Therefore we overcome the aforementioned problem of finding FF values at $t > 0$. Now the experimentally measured FFs can be used directly for the calculation of Eq. (5). Then we calculate the two-photon exchange amplitudes numerically using different FF parametrizations and discuss the results.

[1]Of course, this is a vicious circle, since the accurate FF extraction from experiment implies taking into account the box diagram. However, as a zeroth-order approximation we may neglect it; then some iterative procedure may be used to obtain the precise result.

II. THE METHOD

The box and x-box diagrams, as well as notation for particle momenta, are displayed in Fig. 2. The thin line is for the electron, and the thick line is for proton. The proton and electron masses are M and m, respectively. We also denote

$$P = (p + p')/2,\ K = (k + k')/2,\ q = p' - p. \quad (6)$$

The following relations are fulfilled:

$$q_1 = p'' - p,\ q_2 = p'' - p',\ k'' = K \pm (P - p''), \quad (7)$$

where the upper sign is for the box diagram and the lower for the x-box diagram.

The amplitude corresponding to either diagram is

$$i\mathcal{M}_{\substack{\text{box}\\ \text{x box}}} = \left(\frac{\alpha}{\pi}\right)^2 \times \int \frac{N(p'')\, d^4 p''}{(q_1^2 - \lambda^2)(q_2^2 - \lambda^2)(k''^2 - m^2)(p''^2 - M^2)}, \quad (8)$$

where

$$N(p'') = \bar{u}' \gamma_\mu (\hat{k}'' + m) \gamma_\nu u \cdot \bar{U}' \Gamma_\mu(q_2)(\hat{p}'' + M) \Gamma_\nu(q_1) U, \quad (9)$$

Γ_μ is defined by Eq. (3), and we use the notation $\hat{a} \equiv a_\mu \gamma^\mu$. For the x-box diagram one should interchange γ_μ with γ_ν in Eq. (9). The "photon mass" λ is introduced in the denominator to avoid IR divergence. Though the electron mass is small compared to the characteristic energies involved, we will not neglect it in the denominator, first, for generality, and second, since, as is seen from the result, each of the diagrams diverges like $\ln m$ as $m \to 0$ (but their sum does not).

In the general case elastic *ep* scattering is described by six invariant amplitudes. However, three of them are proportional

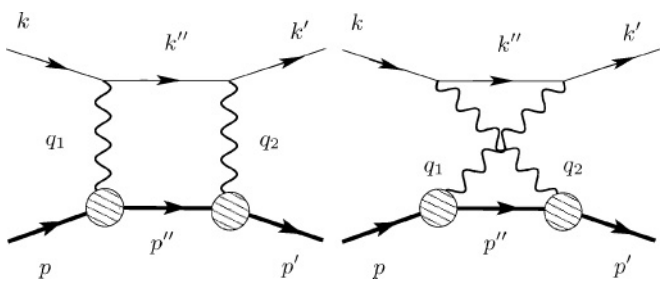

FIG. 2. Box diagram (left) and x-box diagram (right) with the proton in the intermediate state.

to m, so in the $m \to 0$ limit only three remain [7]:

$$\mathcal{M} = \frac{4\pi\alpha}{q^2}\bar{u}'\gamma_\mu u \cdot \bar{U}' \times \left(\tilde{F}_1\gamma^\mu - \tilde{F}_2[\gamma^\mu, \gamma^\nu]\frac{q_\nu}{4M} + \tilde{F}_3\hat{K}\frac{P^\mu}{M^2}\right)U. \quad (10)$$

The invariant amplitudes $\tilde{F}_i$ depend on two kinematic variables, $\nu = 4PK$ and $t = q^2$. In first-order PT, $\tilde{F}_1(\nu, t) = F_1(t)$, $\tilde{F}_2(\nu, t) = F_2(t)$, and $\tilde{F}_3(\nu, t) = 0$. The contribution of the box diagram to any of these amplitudes is given by the integral, similar to Eq. (8), but with another numerator,

$$N(p'') = \sum_{i,j=1}^{2} A_{ij}(p'')F_i\left(q_1^2\right)F_j\left(q_2^2\right), \quad (11)$$

where $A_{ij}(p'')$ are some (rather cumbersome) explicitly known scalar polynomial functions of p''. To simplify the notation, from now on we drop the sum sign and the summation indices in expressions like Eq. (11) and write them simply as $A(p'')F(q_1^2)F(q_2^2)$. However, the summation is always understood.

There are at most four independent scalar functions of p'', say, p''^2, pp'', $p'p''$, and Kp'' (the pseudoscalar combination $\epsilon_{\mu\nu\sigma\tau}p''^\mu p^\nu p'^\sigma K^\tau$ cannot appear because of parity considerations). The alternative, more convenient choice is

$$\begin{aligned} p''^2 - M^2, \\ k''^2 - m^2 = \frac{t_1 + t_2 - t}{2} \pm 2KP \mp 2Kp'', \\ t_1 \equiv q_1^2 = p''^2 + M^2 - 2pp'', \\ t_2 \equiv q_2^2 = p''^2 + M^2 - 2p'p'', \end{aligned} \quad (12)$$

where the upper sign is for the box diagram and the lower for the x-box diagram. Since $A_{ij}(p'')$ are polynomials in p'', they can also be written as polynomials in four variables (12).

Now it is easy to see that the integral (8) can be reduced to the four basic integrals

$$I_n = \int \frac{A(t_1, t_2)\bar{F}(t_1)\bar{F}(t_2)}{D_n}d^4p'', \quad (13)$$

where A is a polynomial, $\bar{F}(t) = F(t)/(t - \lambda^2)$, and

$$\begin{aligned} D_1 &= 1, \\ D_2 &= k''^2 - m^2, \\ D_3 &= p''^2 - M^2, \\ D_4 &= (k''^2 - m^2)(p''^2 - M^2). \end{aligned} \quad (14)$$

If the maximal power of $k''^2 - m^2$ or $p''^2 - M^2$ in $A(p'')$ is greater than one, then other integrals can appear in the decomposition of Eq. (8). However, they are expressed through Eq. (13) by using symmetry considerations (see Appendix A).

For the x-box diagram the integrals I_1, I_2, and I_3 are the same as for the box diagram, but the integral I_4 is not, since the relation between p'' and k'' is different. We denote the corresponding integral I_{4x}.

We will show here in detail the evaluation of the integral I_4. Other integrals are evaluated similarly. At the end we write down the results for all of them.

As it was discussed previously, the idea is to integrate over two of four integration variables to obtain

$$I_n = \int \mathcal{K}_n(t_1, t_2)A(t_1, t_2)\bar{F}(t_1)\bar{F}(t_2)dt_1dt_2, \quad (15)$$

with explicitly known functions $\mathcal{K}_n$. This expression can be used for numerical integration or further analysis.

III. EVALUATION OF κ_n

We will perform the calculation in the Breit frame. In this frame we have

$$\begin{aligned} P &= \left(\frac{1}{2}\sqrt{4M^2 - t}, 0, 0, 0\right), \quad q = (0, 0, 0, \sqrt{-t}), \\ K &= \left(\frac{\nu}{2\sqrt{4M^2 - t}}, \sqrt{\frac{\nu^2 - (4m^2 - t)(4M^2 - t)}{4(4M^2 - t)}}, 0, 0\right) \end{aligned} \quad (16)$$

where the first component is the time component and the following are x, y, and z components). We also let

$$p'' = \left(\xi + \frac{1}{2}\sqrt{4M^2 - t}, \rho\cos\phi, \rho\sin\phi, \eta\right), \quad (17)$$

so $d^4p'' = d\xi d\eta\rho d\rho d\phi$. In this notation

$$\begin{aligned} t_{1,2} &= \xi^2 - \rho^2 - (\eta \pm \sqrt{-t}/2)^2, \\ p''^2 - M^2 &= \left(\xi + \frac{1}{2}\sqrt{4M^2 - t}\right)^2 - \eta^2 - \rho^2 - M^2, \\ k''^2 - m^2 &= \left(\frac{\nu}{2\sqrt{4M^2 - t}} - \xi\right)^2 - \rho^2 - \eta^2 \\ &\quad - m^2 - K_x^2 + 2\rho K_x\cos\phi. \end{aligned} \quad (18)$$

We are to calculate the following integral:

$$I_4 = \int \frac{A(t_1, t_2)\bar{F}(t_1)\bar{F}(t_2)}{(p''^2 - M^2)(k''^2 - m^2)}d\xi d\eta\rho d\rho d\phi. \quad (19)$$

First we integrate over ϕ. The only quantity that does depend on ϕ is k''^2. By using

$$\frac{1}{2\pi}\int_0^{2\pi}\frac{d\phi}{z - \cos\phi} = \frac{1}{\sqrt{z^2 - 1}} \quad (20)$$

it is easy to verify that

$$\begin{aligned} D_\phi &= \left(\frac{1}{2\pi}\int_0^{2\pi}\frac{d\phi}{k''^2 - m^2}\right)^{-1} \\ &= \sqrt{\left(\xi^2 - \frac{\nu}{\sqrt{4M^2 - t}}\xi - \rho^2 - \eta^2 - \frac{t}{4}\right)^2 - 4K_x^2\rho^2}. \end{aligned} \quad (21)$$

In Eq. (20) and further the following convention is used: We mean by $\sqrt{z^2 - a^2}$ the analytic function of z with the branch cut from $-a$ to a such that $\sqrt{z^2 - a^2} > 0$ for $z > a$ and $\sqrt{z^2 - a^2} < 0$ for $z < -a$. Consequently, Eq. (21) implies that, if D_ϕ is real, it has the same sign as the expression in

parentheses under the radical. The integral becomes

$$I_4 = 2\pi \int \frac{A(t_1,t_2)\bar{F}(t_1)\bar{F}(t_2)}{(p''^2 - M^2)D_\phi(\xi,\eta,\rho)} d\xi d\eta\rho d\rho = \int \Phi d\xi d\eta d\rho^2. \quad (22)$$

Next we will integrate over ξ. Here we intend to use Wick rotation, so we need to study the analytic properties of the integrand. The FFs $F(t)$ [and thus $\bar{F}(t)$] are analytic functions of t everywhere in the physical sheet except the positive real axis. Namely, FFs have branch cuts running from $t = (2m_\pi)^2$ to $+\infty$ (where m_π is the pion mass) [8], and the additional pole at $t = \lambda^2$ is due to the photon propagator; the physical value is $\bar{F}(t + i0)$. In the complex ξ plane the corresponding singularities lie at $\xi^2 > \rho^2 + (|\eta| - \sqrt{-t}/2)^2$. The factor $1/(p''^2 - M^2)$ has two poles *1* and *2* at $\xi = -\frac{1}{2}\sqrt{4M^2 - t} \pm \sqrt{\rho^2 + \eta^2 + M^2}$ and D_ϕ has two branch cuts *3* and *4* running from

$$\xi = \frac{\nu}{2\sqrt{4M^2 - t}} \pm \sqrt{(\rho - K_x)^2 + \eta^2 + m^2}$$

to

$$\frac{\nu}{2\sqrt{4M^2 - t}} \pm \sqrt{(\rho + K_x)^2 + \eta^2 + m^2}.$$

When integrating over ξ, we must pass by these singularities, adding $-i0$ to the masses in the usual way. The resulting integration path ℓ is shown in Fig. 3 on the left.

Now we perform the Wick rotation to superpose the integration path with the imaginary axis. If the singularities *1* and *3* lie at $\xi > 0$ and *2* and *4* lie at $\xi < 0$, then the integration path can be rotated without crossing them (Fig. 3, upper drawing). Although singularities *2* and *3* always fulfill this condition, it may not hold for *1* and *4*. In this case extra terms appear when the path crosses the singularities (Fig. 3, lower drawing).

In general case we may write

$$\int_\ell \Phi d\xi = \int_{-i\infty}^{+i\infty} \Phi d\xi + \int \Delta\Phi d\xi \theta(\xi)\theta\left(\frac{\nu}{2\sqrt{4M^2 - t}} - \xi\right) \times \theta\left(-D_\phi^2\right) - 2\pi i \int [(p''^2 - M^2)\Phi]\theta(-\xi) \times \theta\left(\xi + \frac{1}{2}\sqrt{4M^2 - t}\right)\delta(p''^2 - M^2)\, d\xi, \quad (23)$$

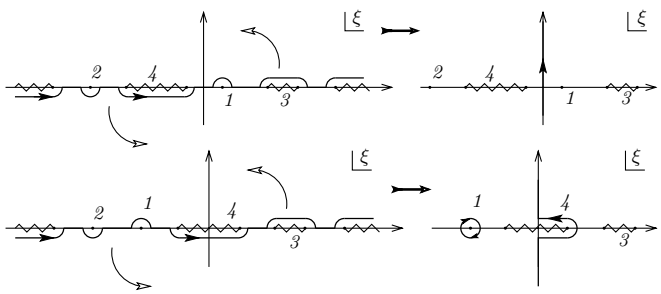

FIG. 3. The integration path before (left) and after Wick rotation (right).

where $\Delta\Phi = \Phi(\xi - i0) - \Phi(\xi + i0) = 2\Phi(\xi - i0)$. During integration of Eq. (23), t_1 and t_2 are always negative. For the first integral on the right-hand side $\xi^2 < 0$ and thus $t_{1,2} = \xi^2 - \rho^2 - (\eta \pm \sqrt{-t}/2)^2 < 0$. As we will see later, the same is true for other integrals. This is a great advantage, since the FFs are well known for $t < 0$ (which corresponds to elastic scattering) but poorly known for $t > 0$.

Here we will change variables to make new independent variables (t_1, t_2, ξ) instead of (ρ, η, ξ). It is important to take into account that $\rho^2 > 0$; for this purpose we insert $\theta(\rho^2)$ under the integral. This implies the condition $\xi^2 > -\frac{t}{4} + \frac{t_1+t_2}{2} - \frac{(t_1-t_2)^2}{4t} = \xi_*^2$, and the integration path along the imaginary axis becomes bounded.

It is convenient to introduce the notation

$$x_\infty = \frac{1}{t}\left(\frac{t_1 + t_2 - t}{2}\right)^2 - \frac{1}{t}t_1t_2,$$
$$x_M = \frac{1}{t}\left(\frac{t_1 + t_2 - t}{2}\right)^2 - \left(\frac{1}{t} - \frac{1}{4M^2}\right)t_1t_2, \quad (24)$$
$$x_m = \frac{1}{t}\left(\frac{t_1 + t_2 - t}{2}\right)^2 - \left(\frac{1}{t} - \frac{1}{4m^2}\right)t_1t_2.$$

Note that at $t_1, t_2 < 0$ one has $x_m > x_M > x_\infty$.

In new variables we have

$$p''^2 - M^2 = \xi\sqrt{4M^2 - t} + \frac{t_1 + t_2 - t}{2} = \sqrt{4M^2 - t}(\xi - \xi_0 - C), \quad (25)$$

$$D_\phi = -\sqrt{4m^2 - t}\sqrt{(\xi - \xi_0)^2 - B^2}, \quad (26)$$

where $\xi_0 = \frac{t_1+t_2-t}{2}\frac{\nu}{(4m^2-t)\sqrt{4M^2-t}}$, $B = \frac{4mK_x}{4m^2-t}\sqrt{x_m}$, and $C = -\frac{t_1+t_2-t}{2\sqrt{4M^2-t}}(1 + \frac{\nu}{4m^2-t})$. Therefore when Φ is expressed through t_1, t_2, and ξ, it has, as a function of ξ, just one pole and one branch cut. It is worth noting that Eq. (26) may differ in sign from D_ϕ defined according to Eq. (21); however, along the integration path they are always equal.

Rewriting Eq. (23) in new variables and after involved algebraic transformations (see Appendix B), we obtain

$$I_4 = -\pi \int_{t_1,t_2 \leqslant 0} \frac{dt_1 dt_2}{2\sqrt{-t}} \frac{A(t_1,t_2)\bar{F}(t_1)\bar{F}(t_2)}{\sqrt{4m^2 - t}\sqrt{4M^2 - t}} \times \left\{\theta(x_\infty)\int_{\ell'} \frac{d\xi}{(\xi - \xi_0 - C)\sqrt{(\xi - \xi_0)^2 - B^2}} + 2i\theta(x_m)\theta(-x_\infty)\theta(t_1 + t_2 - t)\right.$$

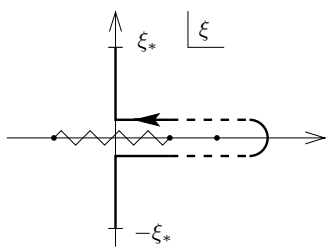

FIG. 4. New integration path ℓ'.

$$\times \int_{\xi_0-B}^{\xi_0+B} \frac{d\xi}{(\xi-\xi_0-C)\sqrt{B^2-(\xi-\xi_0)^2}} - 2\pi i[\theta(x_\infty) + \theta(x_M)\theta(-x_\infty)\theta(t_1+t_2-t)]\frac{1}{\sqrt{C^2-B^2}}\Bigg\}, \quad (27)$$

where ℓ' is the integration path depicted in Fig. 4.

The integration over ξ now can be done analytically. The second integral, after substitution of $\xi = \xi_0 + B\cos\varphi$, is done with the help of Eq. (20) and gives

$$\int_{\xi_0-B}^{\xi_0+B} \frac{d\xi}{(\xi-\xi_0-C)\sqrt{B^2-(\xi-\xi_0)^2}} = \int_0^\pi \frac{d\varphi}{B\cos\varphi - C} = -\frac{\pi}{\sqrt{C^2-B^2}}. \quad (28)$$

The first integral is done using

$$\int \frac{dz}{(z-C)\sqrt{z^2-B^2}} = \frac{1}{2\sqrt{C^2-B^2}} \ln \frac{Cz-B^2-\sqrt{C^2-B^2}\sqrt{z^2-B^2}}{Cz-B^2+\sqrt{C^2-B^2}\sqrt{z^2-B^2}} = \Lambda(z). \quad (29)$$

Here and in the following $\ln z$ is defined with the branch cut from $z = 0$ to $+\infty$, so that for $z > 0$, $\mathrm{Im}\ln(z+i0) = 0$ and $\mathrm{Im}\ln(z-i0) = 2\pi$.

It is easy to show that the argument of the logarithm in Eq. (29) can be real positive only if z is real, so all the discontinuities of $\Lambda(z)$ lie on the real axis. Therefore

$$\int_{\ell'} \frac{d\xi}{(\xi-\xi_0-C)\sqrt{(\xi-\xi_0)^2-B^2}} = \Lambda(\xi_*-\xi_0) - \Lambda(-\xi_*-\xi_0) - \Lambda(+\infty+i0) + \Lambda(+\infty-i0).$$

Using

$$\sqrt{(\xi_*-\xi_0)^2-B^2} = \frac{1}{\sqrt{4m^2-t}} \times \left(\frac{\nu\xi_*}{\sqrt{4M^2-t}} - \frac{t_1+t_2-t}{2}\right), \quad (30)$$

after some simplifications, we arrive at the final result of the form (15) with $\mathcal{K}_4$, which is given here together with other $\mathcal{K}_n$:

$$\mathcal{K}_1(t_1,t_2) = \frac{\pi\xi_*}{\sqrt{-t}}\theta(x_\infty), \quad (31)$$

$$\mathcal{K}_2(t_1,t_2) = \frac{\pi}{2\sqrt{-t(4m^2-t)}}\left\{\theta(x_\infty)\ln\left(\xi+\frac{t_1+t_2-t}{2\sqrt{4m^2-t}}\right)\Bigg|_{-\xi_*}^{\xi_*} - 2\pi i\theta(x_m)\theta(-x_\infty)\theta(t_1+t_2-t)\right\}, \quad (32)$$

$$\mathcal{K}_3(t_1,t_2) = \frac{\pi}{2\sqrt{-t(4M^2-t)}}\left\{\theta(x_\infty)\ln\left(\xi+\frac{t_1+t_2-t}{2\sqrt{4M^2-t}}\right)\Bigg|_{-\xi_*}^{\xi_*} - 2\pi i\theta(x_M)\theta(-x_\infty)\theta(t_1+t_2-t)\right\}, \quad (33)$$

$$\mathcal{K}_4(t_1,t_2) = \frac{\pi}{2\sqrt{R_+}}\left\{\theta(x_\infty)\ln\left[\frac{\xi}{\sqrt{-t}}\sqrt{R_+} - \nu x_\infty + \left(\frac{t_1+t_2-t}{2}\right)^2\right]\Bigg|_{-\xi_*}^{\xi_*} + 2\pi i\theta(x_\infty) + 2\pi i\theta(-x_\infty)\theta(t_1+t_2-t)[\theta(x_m)+\theta(x_M)]\right\}, \quad (34)$$

$$\mathcal{K}_{4x}(t_1,t_2) = \frac{-\pi}{2\sqrt{R_-}}\left\{\theta(x_\infty)\ln\left[\frac{\xi}{\sqrt{-t}}\sqrt{R_-} - \nu x_\infty - \left(\frac{t_1+t_2-t}{2}\right)^2\right]\Bigg|_{-\xi_*}^{\xi_*} + 2\pi i\theta(t_1+t_2-t)[\theta(x_m)\theta(-x_M) + 2\theta(R_-)\theta(x_M)\theta(\nu+t-4M^2)]\right\}, \quad (35)$$

where $\xi_* = i\sqrt{x_\infty}$ and

$$R_\pm = \left(\frac{t_1+t_2-t}{2}\right)^2[(\nu\mp t)^2 - 16m^2M^2] - t_1t_2[\nu^2-(4m^2-t)(4M^2-t)], \quad (36)$$

$\sqrt{R_\pm} = \sigma|R_\pm|^{1/2}$, where $\sigma = -\mathrm{sign}\,(t_1+t_2-t)$ if $R_\pm > 0$ and $\sigma = -i$ if $R_\pm < 0$.

IV. NUMERICAL RESULTS

It is convenient to distinguish three integration regions: (i) $x_\infty \geqslant 0$, (ii) $x_M \geqslant 0 \geqslant x_\infty$, and (iii) $x_m \geqslant 0 \geqslant x_M$. In the general case the integrals I_2, I_4, and I_{4x} contain logarithmic terms like $\ln\frac{m}{\lambda}$ originating from the integration over the $x_m \geqslant 0 \geqslant x_M$ region. However, in actual calculations, after adding box and x-box diagrams, these logarithms always cancel; this can be shown to be the consequence of gauge invariance. Therefore we may put $m = 0$ if the amplitude is evaluated as a whole (box + x box).

Before calculating $ep \to ep$ amplitudes, the following cross-check can be performed. If we omit $A(t_1,t_2)$ and set $F(t) \equiv 1$ in Eq. (13) then the integrals I_n can also be done by the usual Feynman parameters method. We have calculated them numerically with different values of M, m, λ, t, and ν and made sure that both methods give identical results.

Now we turn to evaluation of the invariant amplitudes $\tilde{F}_1$, $\tilde{F}_2$, and $\tilde{F}_3$. Each of them looks like

$$\tilde{F}_i = a_i\ln\lambda + b_i + o(\lambda). \quad (37)$$

The first (IR divergent) term does not contribute to the cross section if the radiation of soft photons is taken into account. To extract both IR divergent and IR finite parts and to simplify the calculation we used the following procedure. We calculated the integrals needed at several small but nonzero λ and fitted obtained values with a three-parameter fit:

$$\tilde{F}_i = a_i\ln\lambda + b_i + c_i\lambda. \quad (38)$$

Though the third term vanishes as $\lambda \to 0$, it turns out to be necessary to obtain accurate results.

The results obtained by Tsai [2] are

$$\tilde{F}_{1,2}^{(T)} = \frac{\alpha}{\pi} F_{1,2}\left[K(p,k') - K(p,k)\right], \quad \tilde{F}_3^{(T)} = 0, \qquad (39)$$

where $K(p_i, p_j) = (p_i \cdot p_j)\int_0^1 \frac{dy}{p_y^2} \ln\frac{p_y^2}{\lambda^2}$, $p_y = p_i y + p_j(1-y)$; the superscript (T) hereafter indicates Tsai's result. In spite of the approximate nature of this result, the terms proportional to $\ln\lambda$ are exact; they are

$$a_{1,2} = a_{1,2}^{(T)} = \frac{2\alpha}{\pi} F_{1,2} \ln\frac{\nu - t}{\nu + t}. \qquad (40)$$

Our numerical calculation has given the same results for these terms.

Instead of $\tilde{F}_{1,2}$ we introduce linear combinations $\tilde{G}_M$ and $\tilde{G}_E$ exactly as is done for the FFs, $\tilde{G}_E = \tilde{F}_1 + \frac{t}{4M^2}\tilde{F}_2$ and $\tilde{G}_M = \tilde{F}_1 + \tilde{F}_2$. To see the relative size of corrections with respect to the Born approximation, we consider the following quantities:

$$\begin{aligned} \delta G_M/G_M &= \left(\tilde{G}_M - G_M^{(T)} - G_M\right)/G_M, \\ \delta G_E/G_M &= \left(\tilde{G}_E - G_E^{(T)} - G_E\right)/G_M, \\ Y_{2\gamma} &= (\nu/4M^2)(\tilde{F}_3/G_M). \end{aligned} \qquad (41)$$

The results of Tsai are subtracted, since they were used (the therefore already taken into account) in the analysis of almost all experimental data. This is not the same as just dropping the logarithmic term, since Eq. (39) contains nonlogarithmic terms as well.

Note that, in contrast to what was done in Ref. [6], we normalize δG_E by G_M, rather than G_E. This is done because of the great discrepancy in G_E as extracted by the two methods; in addition, G_E as extracted by the polarization transfer method is close to zero at $Q^2 \approx 6$ GeV^2 and $\delta G_E/G_E$ becomes large though δG_E itself is small. The uncertainty in G_M is much smaller.

We have calculated the two-photon exchange amplitudes at $Q^2 = 1,3,6,$ and 10 GeV^2 using three FF parametrizations:

(i) a dipole fit,
(ii) a fit from Ref. [9] (under the assumption $G_E/G_M =$ const), and
(iii) a fit from Ref. [10] (to data obtained by polarization transfer).

The results are plotted in Fig. 5 versus the customary parameter (virtual photon polarization) $\varepsilon = \frac{\nu^2 + t(4M^2 - t)}{\nu^2 - t(4M^2 - t)}$.

We see that in general results agree with those obtained in Ref. [6]. This is not surprising, because in Sec. III we actually prove that given the FF parametrization, which is good for the spacelike region ($t < 0$) and has correct analytic properties, the result will not depend on the quality of the fit for $t > 0$ (*a priori* this was not clear). In some sense we justify the approach of Ref. [6]. Nevertheless, our approach is more general, since we can use any FF parametrization.

We also see that the dependence on the choice of FFs is small for $Q^2 < 6$ GeV^2; however, for the generalized electric FF at $Q^2 = 10$ GeV^2 the difference reaches 50% (for small ε).

The absolute value of corrections increases with Q^2 up to $\sim$3% for $\delta G_M/G_M$ at $Q^2 = 10$ GeV^2.

The main purpose of this paper is to present a new approach for evaluation of the two-photon exchange diagram. That is why we will not analyze the effect of these corrections on the FF measurements. Such analysis requires evaluation of bremsstrahlung corrections as well, and thus detailed

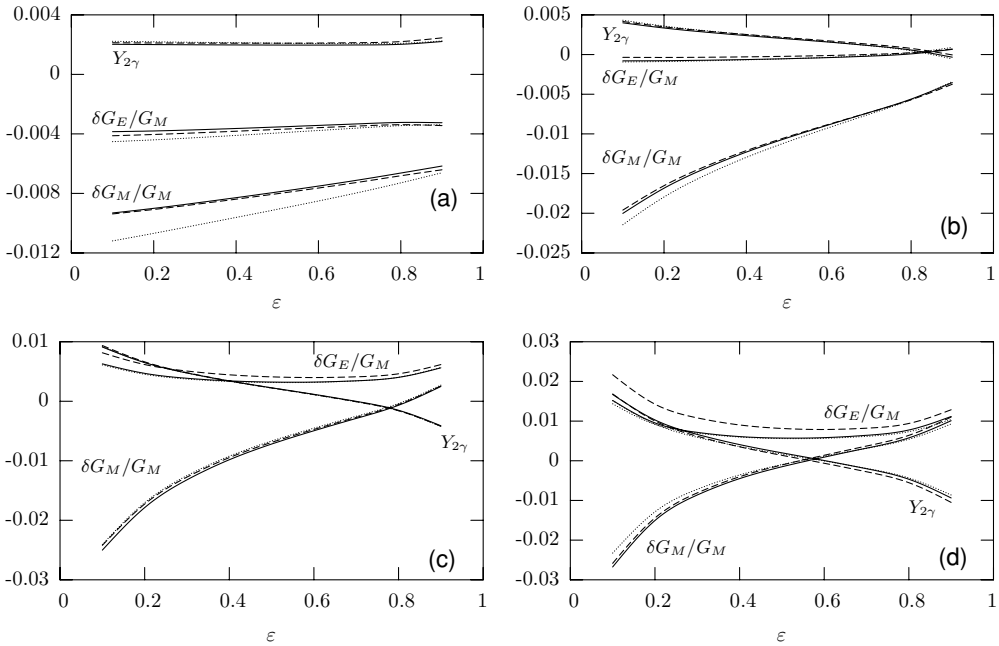

FIG. 5. Two-photon exchange corrections $\delta G_M/G_M$, $\delta G_E/G_M$, and $Y_{2\gamma}$ as indicated on the figures, for Q^2 values of (a) 1 GeV^2, (b) 3 GeV^2, (c) 6 GeV^2, and (d) 10 GeV^2, using form-factor parametrization: from Ref. [9] (solid), from Ref. [10] (dashed), and dipole fit (dotted).

consideration of experimental conditions is needed. We postpone that discussion to another paper.

V. SUMMARY

We study the two-photon exchange in elastic *ep* scattering. In this paper we calculate box and x-box diagrams with the proton in the intermediate state (elastic contribution). Our approach has two main advantages:

(i) The amplitude is expressed via proton form factors in the spacelike region only [Eq. (5)]. The previous calculations required form factors in the timelike region as well, where they are poorly known.
(ii) Any suitable form-factor parametrization in the spacelike region can be used to evaluate the loop integral. In previous calculations only particular kinds of parametrization could be used, since the loop integral was expressed via four-point functions.

A similar approach can be used to evaluate $\Delta(1232)$ and other resonances contributions, which is currently under investigation. At present only the Δ contribution was considered in the literature [11] using the approach of Refs. [5,6] and simple dipole parametrization of the $N \to \Delta$ transition form factors.

We have calculated two-photon exchange amplitudes using form factors as extracted by Rosenbluth separation and by the polarization transfer method. The dependence of the result on the choice of form factors is small except for that of the generalized electric form factor for $Q^2 \geqslant 6\ \mathrm{GeV}^2$.

The same method can be applied to the scattering off any spin-1/2 particle, such as the neutron or ^{3}He.

APPENDIX A

In this Appendix we show how some integrals that can appear in the decomposition of Eq. (8) are reduced to four basic types [Eq. (13)].

Consider the integral

$$\begin{aligned}
&\int A(t_1,t_2)\frac{p''^2-M^2}{k''^2-m^2}d^4p'' \\
&= \int A(t_1,t_2)\frac{(P+K-k'')^2-M^2}{k''^2-m^2}d^4p'' \\
&= \frac{\nu+4m^2-t}{2}\int A(t_1,t_2)\frac{1}{k''^2-m^2}d^4p'' + \int A(t_1,t_2)d^4p'' \\
&- 2(P+K)^\mu \int A(t_1,t_2)\frac{k''_\mu}{k''^2-m^2}d^4p''. \qquad \text{(A1)}
\end{aligned}$$

The first and the second integrals on the right-hand side already have the required form. Since $t_{1,2} = (K \pm q/2 - k'')^2$, the last integral depends only on q^μ and K^μ; thus

$$\int A(t_1,t_2)\tfrac{k''_\mu}{k''^2-m^2}d^4p'' = \alpha q_\mu + \beta K_\mu, \qquad \text{(A2)}$$

where

$$\begin{aligned}
\alpha &= \frac{1}{2t}\int A(t_1,t_2)\frac{t_2-t_1}{k''^2-m^2}d^4p'', \\
\beta &= \frac{1}{4m^2-t}\int A(t_1,t_2)\left(\frac{4m^2-t_1-t_2}{k''^2-m^2}+2\right)d^4p'',
\end{aligned} \qquad \text{(A3)}$$

so finally

$$\begin{aligned}
\int A(t_1,t_2)\frac{p''^2-M^2}{k''^2-m^2}d^4p'' &= \frac{1}{2}\left(1+\frac{\nu}{4m^2-t}\right) \\
&\times \int A(t_1,t_2)\frac{t_1+t_2-t}{k''^2-m^2}d^4p'' \\
&- \frac{\nu}{4m^2-t}\int A(t_1,t_2)d^4p''.
\end{aligned} \qquad \text{(A4)}$$

Similarly, one obtains

$$\begin{aligned}
\int A(t_1,t_2)\frac{k''^2-m^2}{p''^2-M^2}d^4p'' &= \frac{1}{2}\left(1+\frac{\nu}{4M^2-t}\right) \\
&\times \int A(t_1,t_2)\frac{t_1+t_2-t}{p''^2-M^2}d^4p'' \\
&- \frac{\nu}{4M^2-t}\int A(t_1,t_2)d^4p''
\end{aligned} \qquad \text{(A5)}$$

and

$$\begin{aligned}
\int A(t_1,t_2)(k''^2-m^2)d^4p'' &= \int A(t_1,t_2)(p''^2-M^2)d^4p'' \\
&= \int A(t_1,t_2)\frac{t_1+t_2-t}{2}d^4p''.
\end{aligned} \qquad \text{(A6)}$$

APPENDIX B

In this Appendix we show in detail the derivation of Eq. (27).

Let us transform the two last integrals in Eq. (23). It follows from Eq. (21) that if $D_\phi^2 < 0$ then always $\rho^2 > 0$, so $\theta(\rho^2)\theta(-D_\phi^2) = \theta(-D_\phi^2)$, and also

$$\begin{aligned}
D_\phi^2\big|_{\xi=\frac{\nu}{2\sqrt{4M^2-t}}} &= \left(\rho^2+m^2+\eta^2-K_x^2\right)^2 \\
&+ 4K_x^2(m^2+\eta^2) > 0,
\end{aligned} \qquad \text{(B1)}$$

so $\theta[\nu/2\sqrt{4M^2-t}-\xi]$ is constant (either 1 or 0) when $D_\phi^2 < 0$. Therefore

$$\begin{aligned}
&\theta(\rho^2)\theta(\xi)\theta\left(\frac{\nu}{2\sqrt{4M^2-t}}-\xi\right)\theta\left(-D_\phi^2\right) \\
&= \theta(\xi)\theta\left(\frac{\nu}{2\sqrt{4M^2-t}}-\xi_0\right)\theta[B^2-(\xi-\xi_0)^2] \\
&= \theta(\xi)\theta(4m^2-t_1-t_2)\theta(x_m)\theta[B^2-(\xi-\xi_0)^2]. \qquad \text{(B2)}
\end{aligned}$$

$\theta(x_m)$ can be inserted since $0 < B^2-(\xi-\xi_0)^2$ implies $0 < B^2 = (\frac{4mK_x}{4m^2-t})^2 x_m$. Rewriting x_m as

$$\begin{aligned}
\frac{4m^2}{4m^2-t}x_m &= \frac{1}{4m^2-t}\left(\frac{t_1+t_2-4m^2}{2}\right)^2 \\
&+ \frac{1}{t}\left(\frac{t_1-t_2}{2}\right)^2 - m^2
\end{aligned} \qquad \text{(B3)}$$

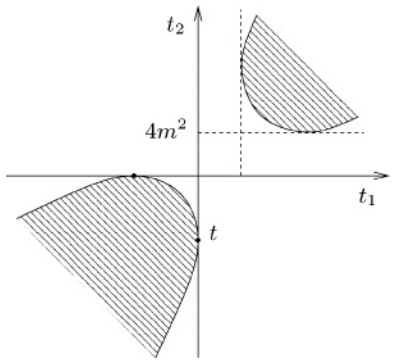

FIG. 6. Regions in (t_1, t_2) plane, where $x_m > 0$ (hatched area).

we can easily see that x_m is positive in two regions, bounded by the hyperbola $x_m = 0$ (Fig. 6). The condition $4m^2 - t_1 - t_2 > 0$ selects the lower-left region, where $t_1, t_2 \leqslant 0$. Thus

$$\theta(4m^2 - t_1 - t_2)\theta(x_m) = \theta(-t_1)\theta(-t_2)\theta(x_m) \tag{B4}$$

and

$$\theta(\rho^2)\theta(\xi)\theta\left(\frac{\nu}{2\sqrt{4M^2 - t}} - \xi\right)\theta\left(-D_\phi^2\right) = \theta(-t_1)\theta(-t_2)\theta(x_m)\theta(\xi)\theta[B^2 - (\xi - \xi_0)^2]. \tag{B5}$$

To transform the last integral, we write

$$\begin{aligned}
&\theta(\rho^2)\theta(-\xi)\theta\left(\xi + \frac{1}{2}\sqrt{4M^2 - t}\right)\delta(p''^2 - M^2) \\
&= \theta(\xi^2 + x_\infty)\theta(-\xi)\theta\left(\xi + \frac{1}{2}\sqrt{4M^2 - t}\right) \\
&\quad \times \delta\left(\xi\sqrt{4M^2 - t} + \frac{t_1 + t_2 - t}{2}\right) \\
&= \theta(x_M)\theta(t_1 + t_2 - t)\theta(4M^2 - t_1 - t_2)\frac{1}{\sqrt{4M^2 - t}} \\
&\quad \times \delta\left(\xi + \frac{t_1 + t_2 - t}{2\sqrt{4M^2 - t}}\right) \\
&= \theta(-t_1)\theta(-t_2)\theta(x_M)\theta(t_1 + t_2 - t)\frac{1}{\sqrt{4M^2 - t}} \\
&\quad \times \delta\left(\xi + \frac{t_1 + t_2 - t}{2\sqrt{4M^2 - t}}\right).
\end{aligned} \tag{B6}$$

The last equality was obtained by using Eq. (B4) with m replaced by M. Again we have $t_1, t_2 \leqslant 0$.

After that, the integral I_4 becomes

$$\begin{aligned}
I_4 = \int\limits_{t_1,t_2\leqslant 0} \frac{dt_1 dt_2}{2\sqrt{-t}} \Bigg\{ &\int_{-i\infty}^{+i\infty} \theta(\xi^2 + x_\infty)\Phi d\xi + \theta(x_m) \\
&\times \int \Delta\Phi d\xi\theta(\xi)\theta[B^2 - (\xi - \xi_0)^2] \\
&- \frac{2\pi i}{\sqrt{4M^2 - t}}\theta(t_1 + t_2 - t)\theta(x_M) \\
&\times \int [(p''^2 - M^2)\Phi]\delta\left(\xi + \frac{t_1 + t_2 - t}{2\sqrt{4M^2 - t}}\right) d\xi \Bigg\}.
\end{aligned} \tag{B7}$$

Now we introduce the integration path ℓ' that passes by the singularities on the right (Fig. 4). After that,

$$\begin{aligned}
\int_{-i\infty}^{+i\infty} \theta(\xi^2 + x_\infty)\Phi d\xi = \theta(x_\infty) \Bigg\{ &\int_{\ell'} \Phi d\xi - \int \Delta\Phi d\xi\theta(\xi) \\
&\times \theta[B^2 - (\xi - \xi_0)^2] - 2\pi i \\
&\times \theta(\xi_0 + C) \int [(\xi - \xi_0 - C)\Phi] \\
&\times \delta(\xi - \xi_0 - C) d\xi \Bigg\}.
\end{aligned} \tag{B8}$$

Combining this with the previous equation, we have

$$\begin{aligned}
I_4 = \int\limits_{t_1,t_2\leqslant 0} \frac{dt_1 dt_2}{2\sqrt{-t}} \Bigg\{ &\theta(x_\infty) \int_{\ell'} \Phi d\xi + \theta(x_m)\theta(-x_\infty) \\
&\times \int \Delta\Phi\theta(\xi)\theta[B^2 - (\xi - \xi_0)^2] d\xi - 2\pi i[\theta(x_\infty) \\
&\times \theta(t - t_1 - t_2) + \theta(x_M)\theta(t_1 + t_2 - t)] \\
&\times \int [(\xi - \xi_0 - C)\Phi]\,\delta(\xi - \xi_0 - C) d\xi \Bigg\}.
\end{aligned} \tag{B9}$$

To proceed further, we note that

$$\begin{aligned}
B^2 - (\xi - \xi_0)^2\big|_{\xi=0} = &\frac{\nu^2}{(4m^2 - t)(4M^2 - t)} x_\infty \\
&- \frac{4m^2}{4m^2 - t} x_m < 0
\end{aligned} \tag{B10}$$

for $x_\infty < 0$ and $x_m > 0$. Therefore

$$\begin{aligned}
&\theta(x_m)\theta(-x_\infty)\theta(\xi)\theta[B^2 - (\xi - \xi_0)^2] \\
&\quad = \theta(x_m)\theta(-x_\infty)\theta(\xi_0)\theta[B^2 - (\xi - \xi_0)^2] \\
&\quad = \theta(x_m)\theta(-x_\infty)\theta(t_1 + t_2 - t)\theta[B^2 - (\xi - \xi_0)^2].
\end{aligned} \tag{B11}$$

Also

$$\begin{aligned}
&\theta(x_\infty)\theta(t - t_1 - t_2) + \theta(x_M)\theta(t_1 + t_2 - t) \\
&\quad = \theta(x_\infty) + [\theta(x_M) - \theta(x_\infty)]\theta(t_1 + t_2 - t) \\
&\quad = \theta(x_\infty) + \theta(x_M)\theta(-x_\infty)\theta(t_1 + t_2 - t)
\end{aligned} \tag{B12}$$

and finally

$$\begin{aligned}
I_4 = \int\limits_{t_1,t_2\leqslant 0} \frac{dt_1 dt_2}{2\sqrt{-t}} \Bigg\{ &\theta(x_\infty) \int_{\ell'} \Phi d\xi + \theta(x_m)\theta(-x_\infty) \\
&\times \theta(t_1 + t_2 - t) \int \Delta\Phi\theta[B^2 - (\xi - \xi_0)^2] d\xi \\
&- 2\pi i[\theta(x_\infty) + \theta(x_M)\theta(-x_\infty)\theta(t_1 + t_2 - t)] \\
&\times \int [(\xi - \xi_0 - C)\Phi]\,\delta(\xi - \xi_0 - C) d\xi \Bigg\}.
\end{aligned} \tag{B13}$$

Substituting, according to Eq. (22),

$$\Phi = \frac{-\pi A(t_1, t_2)\bar{F}(t_1)\bar{F}(t_2)}{\sqrt{4m^2 - t}\sqrt{4M^2 - t}} \frac{1}{(\xi - \xi_0 - C)\sqrt{(\xi - \xi_0)^2 - B^2}}, \tag{B14}$$

$$\Delta\Phi = \frac{-\pi A(t_1, t_2)\bar{F}(t_1)\bar{F}(t_2)}{\sqrt{4m^2 - t}\sqrt{4M^2 - t}} \frac{2i}{(\xi - \xi_0 - C)\sqrt{B^2 - (\xi - \xi_0)^2}}, \tag{B15}$$

into (B13), we obtain Eq. (27).

[1] M. K. Jones *et al*., Phys. Rev. Lett. **84**, 1398 (2000); O. Gayou *et al*., *ibid*. **88**, 092301 (2002); V. Punjabi *et al*., Phys. Rev. C **71**, 055202 (2005); **71**, 069902(E) (2005).
[2] Y. S. Tsai, Phys. Rev. **122**, 1898 (1961).
[3] L. C. Maximon and J. A. Tjon, Phys. Rev. C **62**, 054320 (2000).
[4] Yu. M. Bystritskiy, E. A. Kuraev, and E. Tomasi-Gustafsson, hep-ph/0603132.
[5] P. G. Blunden, W. Melnitchouk, and J. A. Tjon, Phys. Rev. Lett. **91**, 142304 (2003).
[6] P. G. Blunden, W. Melnitchouk, and J. A. Tjon, Phys. Rev. C **72**, 034612 (2005).
[7] P. A. M. Guichon and M. Vanderhaeghen, Phys. Rev. Lett. **91**, 142303 (2003).
[8] S. Gasiorowicz, *Elementary Particle Physics* (Wiley, New York, 1966).
[9] P. E. Bosted, Phys. Rev. C **51**, 409 (1995).
[10] E. J. Brash, A. Kozlov, S. Li, and G. M. Huber, Phys. Rev. C **65**, 051001(R) (2002).
[11] S. Kondratyuk, P. G. Blunden, W. Melnitchouk, and J. A. Tjon, Phys. Rev. Lett. **95**, 172503 (2005).